Application of Adaptive Neuro-Fuzzy Inference System for Prediction of Surface Roughness in Incremental Sheet Metal Forming Process

Aws K. Ibrahim
Production & Materials Engineering Department, University of Technology/Baghdad
Dr. Wisam K. Hamdan
Production & Materials Engineering Department, University of Technology/Baghdad
Email:uot_techmagaz@yahoo.com

Received on:22/6/2014 & Accepted on:8/1/2015

ABSTRACT

In manufacturing processes, surface finish of a product is very crucial in determining the quality. Therefore, the surface quality including the surface roughness is still the most important obstacles against the incremental sheet metal forming (ISMF) process. As a consequence, the possibility to predict the surface roughness values in incremental forming and to correlate these values with the forming parameters can be useful in order to control this important target. Accordingly, an adaptive neuro-fuzzy inference system (ANFIS) is used to predict the surface roughness of parts produced by single-point incremental forming (SPIF) process. The hybrid learning algorithm is applied in ANFIS to determine the most suitable membership functions (MFs) and to simultaneously find the optimal premise and consequent parameters by directly minimizing the root mean squared error (RMSE) as a performance criterion. In order to achieve this target, five forming parameters, namely (tool diameter, incremental step size, tool shape, rotational speed and slope angle) are studied to form pyramid like shapes for the purpose of roughness measurement. Experimental results show that the difference sigmoidal MF gives the minimum RMSE. The predicted surface roughness values using ANFIS are compared with actual data. The comparison indicates that the utilization of difference sigmoidal MF in ANFIS could achieve a satisfactory prediction accuracy using both training and testing data when this MF is adopted. The training and testing prediction accuracy are 95.972% and 85.799% respectively.

Keywords: Adaptive neuro-fuzzy inference system (ANFIS), Incremental sheet metal forming (ISMF), Single-point incremental forming (SPIF), Membership function (MF), Root mean squared error (RMSE).

تطبيق نظام ذكي للتنبؤ بالخشونة السطحية في عملية التشكيل التزايدية للصفائح المعدنية

الخلاصة

يعتبر الانهاء السطحي امر بالغ الاهمية في تحديد جودة المنتجات لأي عملية تصنيعية. وبالتالي فان جودة الاسطح بما في ذلك الخشونة السطحية لا تزال اهم العقبات التي تواجه عملية التشكيل التزايدية للصفائح المعدنية

(ISMF). نتيجة لذلك، فان امكانية التنبؤ بقيم الخشونة السطحية في عملية التشكيل التزايدية وربط تلك القيم مع متغيرات التشكيل يمكن ان تكون مفيدة من اجل تحقيق هذا الهدف الهام. وفقا لذلك، تم استخدام نظام (ANFIS) للتنبؤ بالخشونة السطحية للأجزاء المصنعة باستخدام عملية التشكيل التزايدية المنفردة (SPIF). ومن اجل تحقيق هذا الهدف، تم دراسة خمس عوامل تشكيل وهي (قطر اداة التشكيل، حجم الخطوة، شكل الاداة، السرعة الدورانية وزاوية الميل) وذلك لتشكيل منتجات هرمية الشكل لغرض قياس الخشونة. تمت مقارنة قيم الخشونة السطحية التي تم التنبؤ بها باستخدام (ANFIS) مع القيم الحقيقية حيث بينت النتائج امكانية الحصول على دقة تنبؤ بمقدار 95,972 % و 85,799 % باستخدام كلا من بيانات تكوين واختبار هذا النموذج على التوالي.

INTRODUCTION

In manufacturing industries, surface finish of a product is very crucial in determining the quality. Surface finish is important in terms of tolerances, it reduces assembly time and avoids the need for secondary operation, thus reduces operation time and leads to overall cost reduction. Besides, good-quality surface is significant in improving the performance such as fatigue strength, corrosion resistance, and creep life. Surface roughness also affects several functional attributes of parts, such as contact causing surface friction, wearing, light reflection, heat transmission, ability of distributing and holding a lubricant, load bearing capacity, coating or resisting fatigue. Surface roughness plays an important role in affecting friction, wear and lubrication of contacting bodies. Surface roughness of the contacting surfaces influences the frictional properties of those surfaces during the forming processes [1].

Studying the roughness of parts obtained by single-point incremental forming (SPIF) is necessary and important for the reasons mentioned before. However, surface finish in ISMF is not always preferred to be at its smallest value as in the knee articular surface. In this case, firstly, it is necessary to have an articular (outer) surface that is as smooth as possible, with the smallest possible roughness, in order to avoid affecting the tribological conditions within the joint and, secondly, because the inner surface (the surface that actually comes into contact with the forming tool) has to be as rough as possible in order to provide the best possible adherence to the surface of the bone and of the cartilage [2]. Therefore, the possibility to predict the surface roughness in incremental forming can be useful in order to control this important target. Accordingly, an adaptive neuro-fuzzy inference system (ANFIS) is used to predict the surface roughness of parts produced by SPIF process.

Overview of Single-Point Incremental Forming (SPIF) Process:

In the modern world of manufacturing, the demand of extremely customized products is increasing every day. Even if the mass production is employed until now, the small quantity batches are more and more desired. The key words of manufacturing are: flexibility, product customization, customer orientation, high quality, low production cost. In sheet metal forming, the manufacturing processes evolution towards a more flexible production has made huge steps in the last few years [3].

Today, many industrial sections utilize forming processes such as deep drawing and stamping in order to produce sheet metal parts with high productivity. These processes need large initial investments and long die-preparation times, with special dies for each part, particularly when the parts have complex shapes or are only needed in small batches. Therefore, there is a need for a flexible technology that is also capable of performing small and medium-sized projects [4]. In order to meet these demands, new sheet metal forming techniques, such as incremental sheet

forming (ISF), have been recently introduced, with the aim of minimizing the manufacturing costs and product launch time when small batches or prototypes have to be realized. These sheet metal forming methods reduce the time and the costs for machine tooling replacing at least one of the two dies with the action of a simple tool [5]. SPIF is an innovative and flexible sheet metal-forming technology that uses layered manufacturing basis. It transforms the part geometry information into a group of parameters of 2D layers, and then the plastic-local deformation is done layer-by-layer through the computer numerically controlled movements of a simple forming tool to manufacture products with complex shapes as shown in figure (1) [6].

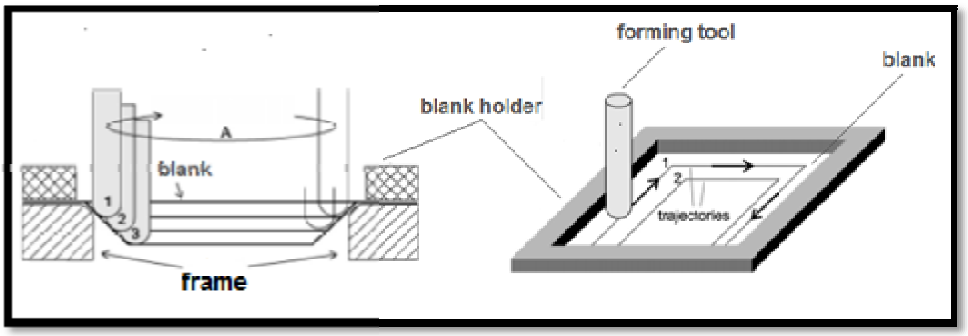

Figure (1): Schematic representation of the SPIF process [7].

Experimental run

This section mainly includes two directions, the first one is manufacturing and preparation of some specific equipment necessary for experimental run. The second direction is the experimental campaign.

Experimental Setup and Equipments

ISMF process is characterized by using very simple equipments in addition to utilized CNC milling machine compared with other sheet forming methods that have utilized punches and dies specific to one shape and size of the final product. These equipments are: CNC milling machine, forming frame, forming tools and sheet material.

CNC Milling Machine

In this work, the experimental campaign has been carried out on three-axis vertical milling machine "C-tek" model "KM-80D" 2008 as shown in Figure (2).

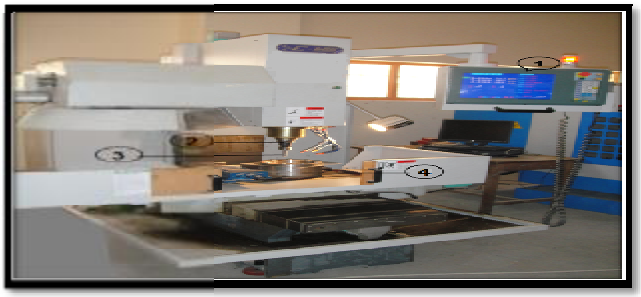

Figure (2): CNC milling machine used in the experimental campaign (1) machine controller, (2) tool holder, (3) forming tool, (4) forming frame.

Forming Frame

The hollow cylindrical frame is manufactured from medium carbon steel by metric turning machine with outer diameter (200 mm) and inner diameter (170 mm) and height of (200mm). A ring with radii equals to the radii of the forming frame has been used as a blank holder. As shown in Figure (3), the blank holder has nine holes distributed uniformly along the circumference of the frame and the blank holder. Nine studs (M8) are utilized in order to fix the blank sheet between the frame and the blank holder.

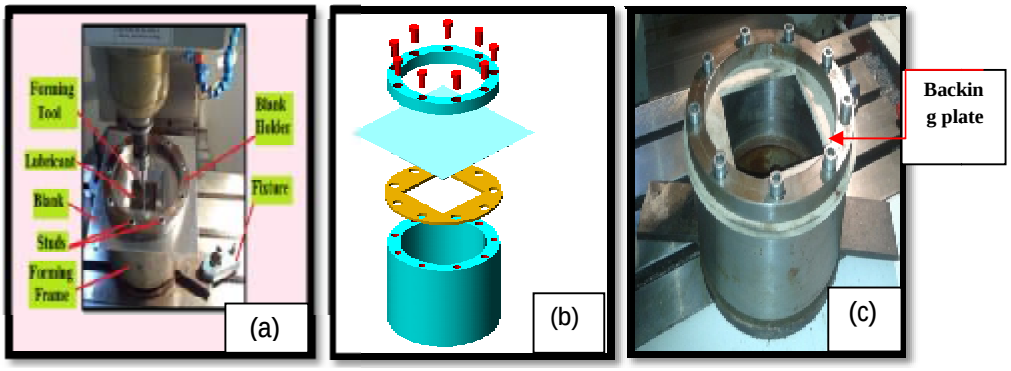

Figure (3): The forming structure used for experiments, (a) SPIF process scope, (b) graphical representation, (c) physical forming frame and blank holder with backing plate that used.

A piece of wood is utilized as a backing plate between the sheet metal blank and the forming frame in order to support the blank while forming and to compensate the lack of shape matching between the square top-view of the pyramid product and the circular opening of both the forming frame and the blank holder. The backing plate has an outer-circular shape with (230) mm diameter and an inner-square shape with dimensions (114x114) mm. The inner shape represents the working area as showr in Figure (3-b & c).

Forming Tools and Sheet Blank

In ISMF process, the cylindrical tool with a ball head, hemispherical or toroidal head is used instead of cutting tool that is used in milling machine. The forming tool is clamped with the tool holder through the chuck of the conical portion. The chuck is cleave to the machine head due to pneumatic pressure system.

In this work, four tools with hemispherical and toroidal heads with diameters (12 & 20 mm) for each type are utilized in order to form the sheet metal according to tool path generation as shown in Figure (4-a & b). The length of each forming tool is 110 mm. All the tools are manufactured from carbon steel AISI 1060. In order to increase the hardness, the forming tools are heat treated to 820 C^0 and quenched in water. In order to get stress relief, the tools are tempered to 200 C^0 and then cooled in open air. The final operation regarding tools is the surface finishing for achieving the best possible smoothness at the tool tip. The tools have been finished using a suitable finishing paper.

In all experiments carried out, sheet metals of an Aluminum alloy AA 1050 are used. The initial size of the sheet is 250x250x0.9 mm, while the working area with diameter 170 mm according to the blank holder size is shown in Figure (4-c) below.

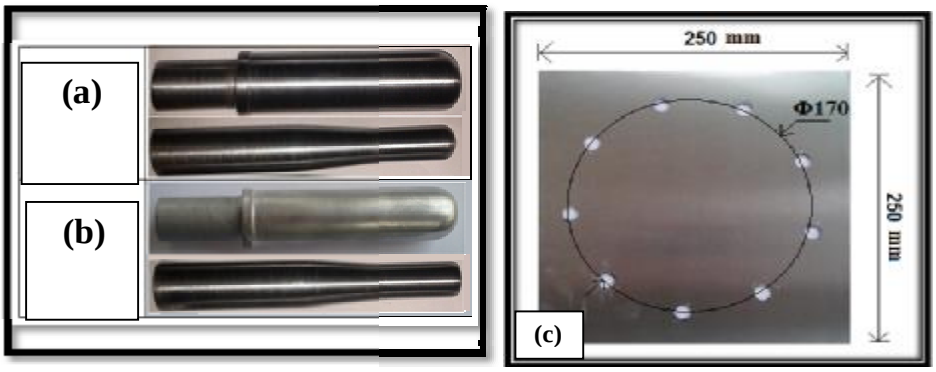

Figure (4): Forming tools and sheet blank that used in experimental campaign; (a) Hemispherical head tool, (b) Toroidal head tool, (c) Sheet blank.

Experimental Campaign

Forming parameters

In this work, the forming parameters are (tool diameter "D", incremental step size "ΔZ, tool shape "S", rotational speed "ω" and slope angle "α"). The incremental step-down size (ΔZ) is the amount of material deformed for each revolution of the forming tool. While the spindle rotational speed is the speed at which the tool rotates. The spindle speed varies the heat generated at the contact point between the material and the forming tool. Slope angle is the angle between the horizontal, undeformed sheet metal and the inclined deformed one as shown in Figure (5).

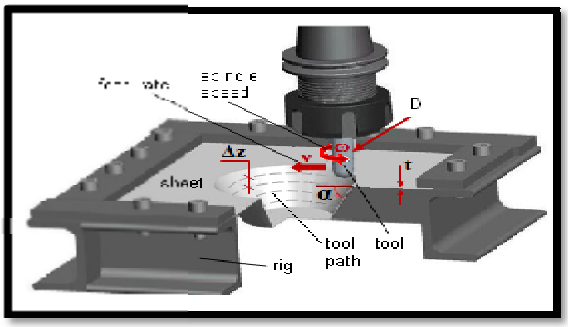

Figure (5): SPIF process parameters [8].

Regarding tool shape parameter, hemispherical and toroidal head tools are used. Toroidal tool has two radii at the tip: major and minor, while the hemi-spherical head tool has one radius as shown in Figure (6).

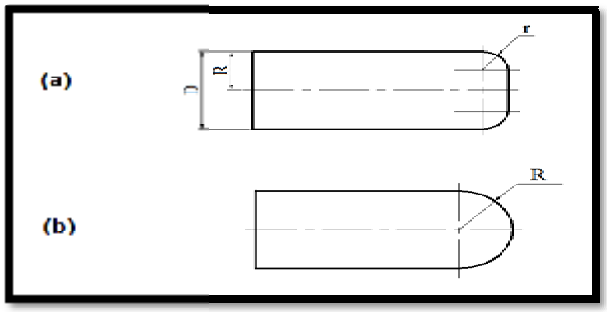

Figure (6): Sketch of forming tools that used: (a) Toroidal end tool, (b) hemispherical end tool.

The shape of toroidal tool (S) can be recognized as the ratio of the minor radius (r) to the major radius (R) of the forming tool as follows:

$$S = \frac{r}{R} \quad \text{.... (1)}$$

In hemispherical head tools, the major and minor radii are equal, therefore the shape value (S) for this type of tool is equal to one as shown in Figure (6). The values of radii and shapes for hemispherical and toroidal tools utilized in this study are identified as given in Table (1).

Table (1): Forming tool shapes that used

Tool type	R (mm)	r (mm)	S
Toroidal	6	2.25	0.375
	10	6	0.6
Hemispherical	6	6	1
	10	10	1

The entire forming parameters that used in this experimental campaign are shown in table (2). With regard to the linear movement of the forming tool, the feed rate is kept constant (600 mm/min) for all experiments that have been carried out.

Table (2): The proposed forming Parameters and their levels.

No.	Parameter	Unit	Levels			
1	Tool Diameter (D)	mm	12		20	
2	Incremental Step Down (ΔZ)	mm	0.1		0.4	1.1
3	Tool Shape (S)	----	0.375		0.6	1
4	Rotational Speed (ω)	r.p.m	800		1400	
5	Slope Angle (α)	Degree	44	49	54	59
6	Feed Rate (F)	mm/min	600			

In this experimental campaign, a full design of experiment that involves all possible physical combinations of variables is created using the control parameters shown in Table (2). In order to reduce the number of the required experiments, a detour way is proposed concerning the geometry of the part. The detour way proposes that each part geometry contains four different angles as it will discussed later in

section (3.2.2). Accordingly, the factor "slope angle" explained in Table (2) can be regarded as a factor of single level instead of four levels. This process reduces the number of trials from 96 to 24 experiments.

Geometry of Parts and Tool Path

The geometry of the formed part is an asymmetric truncated pyramid with total depth of (40mm) for all products as shown in Figure (7). This geometry is kept constant during all the twenty four runs.

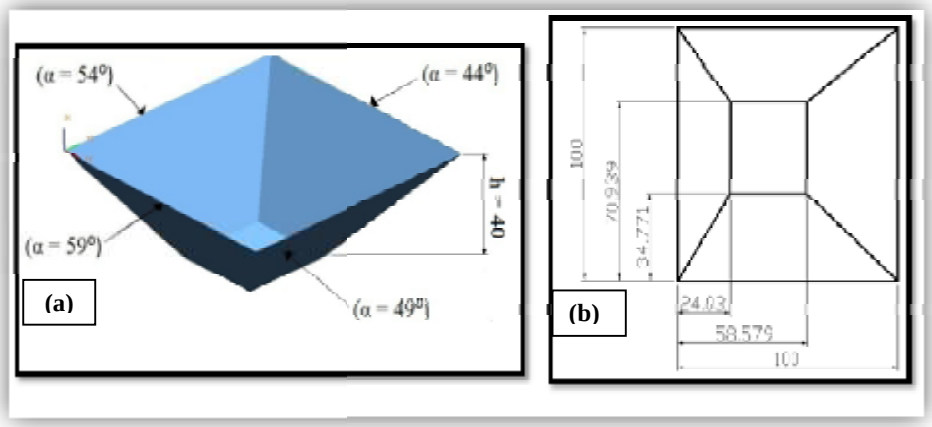

Figure (7): Dimensions details of the product that used: (a) 3D CAD model, (b) Top view.

The CAD model of the product shown before is created by using Siemens UGS-NX5 CAD/CAM software.

In Incremental Forming, the tool motion is controlled numerically. Therefore, all parts were modeled, and a Z-level with constant ΔZ called "Iso-planar" tool path is generated for all products using (Siemens UGS-NX5) CAD/CAM software. The tool path starts from the outside of the shape towards the inner sides and incrementally goes down in the Z-direction by a constant (ΔZ) value as shown in Figure (8). NC codes are obtained from the generated tool path and transferred to the CNC machine.

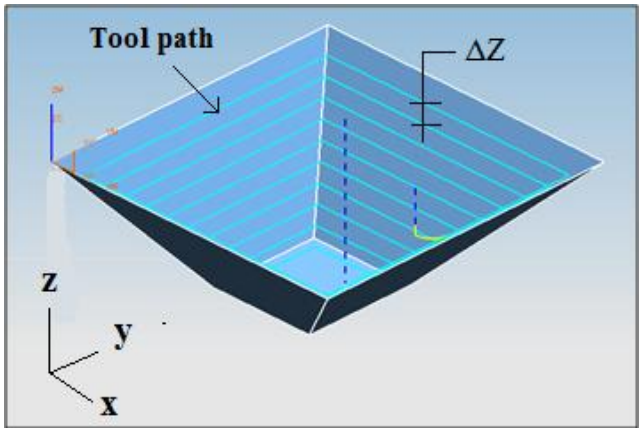

Figure (8): Iso-planar tool path generation using UGS-NX5 software.

The final product is shown in Figure (9) below.

Figure (9): Different views of the final pyramid like shape product.

Surface Roughness Measurement

The surface quality including the surface roughness is still the most important obstacle against ISMF process. As a result; the average roughness R_a has been examined by using a portable surface roughness tester brand "Mahr POCKET SURF ® III" with (0.01 µm) accuracy as shown in Figure (10). R_a is measured because it is widely used as a parameter for surface finishing.

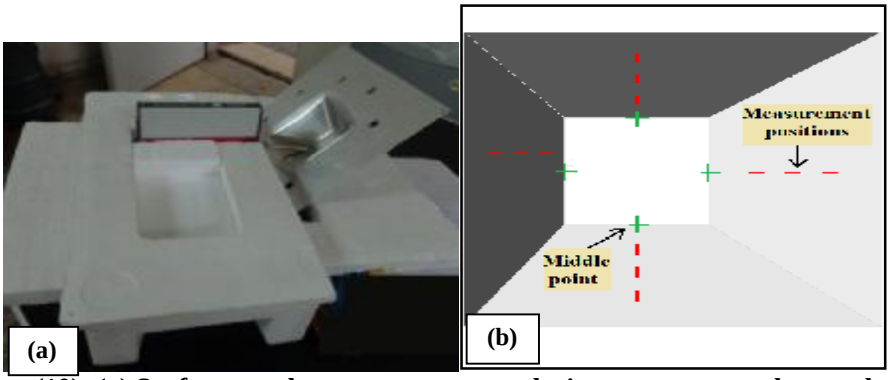

Figure (10): (a) Surface roughness measurement device arrangement that used in experimental campaign, (b) Positions of measurement lines.

A full experimental campaign is carried out for each part. The measurement line is 5 mm long that is based on the probe movement. Three line measures are recorded along each internal face of the pyramids in order to avoid the errors associated with any anisotropic behavior in terms of sheet roughness.

Some surfaces are measured at different positions on the same depth line and the observed differences are (±0.03 µm). Therefore, all measurement lines are recorded at approximately the middle of each side width of the product base except the surfaces that have the incremental line as shown in figure (figure 10-b). The surface roughness has been measured perpendicular to the tool feed direction as shown in Figure (10-a).

The mean of the three measurement lines of the average roughness (R_a) is taken for each surface of all products. The entire matrix results layout according to the full design of experiments and the corresponding mean response roughness are listed in Table (3).

Table (3): The layout of results matrix according to the full design of experiments.

Expt. No.	D (mm)	ΔZ (mm)	S	ω (r.p.m)	Mean Roughness R_a (μm)/ slope angle (α)			
					44°	49°	54°	59°
1	12	0.1	0.375	800	1.08	0.84	0.74	0.60
2	12	0.1	0.375	1400	0.52	0.46	0.39	0.24
3	12	0.1	1	800	0.72	0.64	0.42	0.44
4	12	0.1	1	1400	0.40	0.31	0.24	0.21
5	12	0.4	0.375	800	1.27	1.03	0.78	0.68
6	12	0.4	0.375	1400	1.17	0.68	0.59	0.60
7	12	0.4	1	800	0.77	0.69	0.54	0.43
8	12	0.4	1	1400	0.67	0.52	0.42	0.38
9	12	1.1	0.375	800	3.07	2.51	2.08	1.42
10	12	1.1	0.375	1400	4.30	3.31	1.60	1.58
11	12	1.1	1	800	1.67	1.41	1.27	1.30
12	12	1.1	1	1400	2.21	1.85	1.46	1.30
13	20	0.1	0.6	800	0.45	0.43	0.31	0.31
14	20	0.1	0.6	1400	0.37	0.36	0.27	0.24
15	20	0.1	1	800	0.30	0.27	0.26	0.20
16	20	0.1	1	1400	0.25	0.23	0.21	0.18
17	20	0.4	0.6	800	0.58	0.45	0.40	0.33
18	20	0.4	0.6	1400	0.57	0.42	0.38	0.31
19	20	0.4	1	800	0.39	0.32	0.30	0.25
20	20	0.4	1	1400	0.34	0.32	0.28	0.25
21	20	1.1	0.6	800	1.32	1.20	1.07	0.94
22	20	1.1	0.6	1400	1.40	1.21	1.13	0.90
23	20	1.1	1	800	0.84	0.73	0.75	0.49
24	20	1.1	1	1400	1.23	0.88	0.74	0.56

Modeling of Adaptive Neuro-Fuzzy Inference System (ANFIS)

The adaptive network based fuzzy inference system (ANFIS) is a fuzzy inference system implemented in the framework of an adaptive neural network and it is a useful approach for the solution of function approximation problems [9, 10]. An ANFIS gives the mapping relation between the input and output data by using hybrid learning method to determine the optimal distribution of membership functions. Fuzzy logic is

used in ANFIS in the architecture of a neural network. Such framework makes the ANFIS modeling more systematic and less reliant on expert knowledge [9].

Basically, five network layers are used by ANFIS to perform the following fuzzy inference steps: (i) Input fuzzification, (ii) Fuzzy set database construction, (iii) Fuzzy rule base construction, (iv) Decision making, and (v) Output defuzzification [10].

Each ANFIS layer consists of several nodes described by the node function. The inputs of present layers are obtained from the nodes in the previous layers [9]. To illustrate the procedures of an ANFIS, for simplicity, it is assumed that two inputs (x, y) with two MFs for each input and one output (f_i) are used in this system. The rule base of ANFIS contains fuzzy if-then rules of Sugeno type. For a first order two-rule Sugeno fuzzy inference system, the two rules may be expressed as:

Rule 1: If x is A_1 and y is B_1 then $f_1 = p_1x + q_1y + r_1$ ....(2)

Rule 2: If x is A_2 and y is B_2 then $f_2 = p_2x + q_2y + r_2$ ....(3)

where

x and y are the inputs of ANFIS, A_i , B_i are the fuzzy sets of the inputs, f_i (x, y) is a first order polynomial and represents the outputs of the first order Sugeno fuzzy inference system, p_i ,q_i , r_i are the parameters set, referred to as the consequent parameters. Adaptive nodes, denoted by squares, represent the parameter sets that are adjustable in these nodes, whereas fixed nodes, denoted by circles, represent the parameter sets that are fixed in the system. The architecture of ANFIS is shown in Figure (11) and the node function in each layer is described below [9, 10].

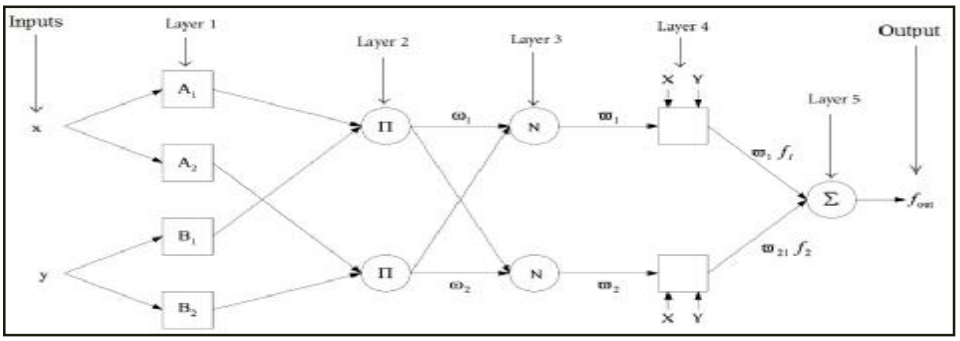

Figure (11): ANFIS architecture for two inputs [10].

Layer1: Calculating the membership value for the Premise parameter

This layer includes adaptive nodes which produce membership grades of an input parameter with node functions defined as:

$O_{l,i} = \mu_{Ai}(x)$ *for i=1,2,* ....(4)

$O_{l,i} = \mu_{Bi-2}(y)$ *for i=3, 4* ....(5)

Where

x and y are the inputs to the node i; A_i and B_{i-2} are the linguistic fuzzy sets related to this node, $O_{l,i}$ is the MFs (μ_{Ai} and μ_{Bi-2}) grade of fuzzy sets and it determines the

degree to which the given input (*x* or *y*) satisfies the quantifier. A generalized difference sigmoidal MF is utilized and can be expressed as (Figure (12)):

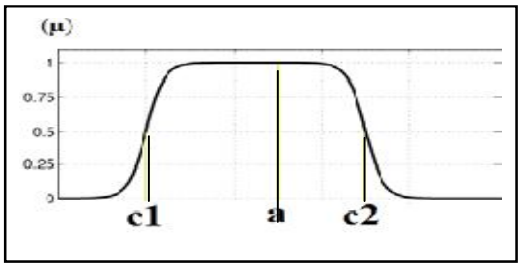

Figure (12): Difference sigmoidal MF.

$$\mu_{Ai}(x) = \frac{1}{1+e^{-a(x-c)}} \quad \text{....(6)}$$

Where

c locates the distance from the origin and ***a*** determines the steepness of the function. A difference sigmoidal MF is formed by the difference between two sigmoidal MFs with parameters (a_1 , c_1) and (a_2, c_2) for each one of them.

Layer 2: Computing of Firing Strength (weight) of Rules

Every node in this layer is a fixed node, marked by a circle and labeled Π, whose output is the product of all incoming signals:

$$O_{2,i} = \omega_i = \mu_{Ai}(x)\,\mu_{Bi}(y) \quad for\ i = 1, 2 \quad \text{...(7)}$$

The output ω_i represents the firing strength (weight) of a rule.

Layer 3: Normalizing of Firing Strength

Every node in this layer is a fixed node, marked by a circle and labeled N, with the node function to normalize the firing strength by calculating the ratio of the i^{th} node firing strength to the sum of all rules' firing strengths as given below:

$$O_{3,i} = \varpi = \frac{\omega i}{\sum \omega i} = \frac{\omega i}{\omega 1+\omega 2} \quad \text{.....(8)}$$

Where

ϖ is called the normalized weighting factor.

Layer 4: Consequent Parameters

Every node in this layer is an adaptive node, marked by a square, with node function:

$$O_{4,i} = \varpi_i f_i = \varpi_i (p_i x + q_i y + r_1) \quad \text{.....(9)}$$

Where

f_i is the output of the i^{th} rule and p_i, q_i r_i are the parameters set, referred to as the consequent parameters.

Layer 5: Overall Output

The single node in this layer is a fixed node labeled Σ, with node function to compute the overall output by summation of all incoming signals:

Overall output (f_{out}) $= O_{5,i} = \Sigma\, \varpi_i f_i$ ....(10)

From ANFIS structure mentioned before, the overall output can be stated as a linear combination of the consequent parameters. The final output O_t can be written as:

$$O_t = \varpi_1 f_1 + \varpi_2 f_2 = \frac{\omega 1}{\omega 1+\omega 2} f_1 + \frac{\omega 2}{\omega 1+\omega 2} f_2$$
$$= p_1(\varpi_1 x) + q_1(\varpi_1 y) + r_1(\varpi_1) + p_2(\varpi_2 x) + q_2(\varpi_2 y) + r_2(\varpi_2) \quad ....(11)$$

Fuzzy inference system must be optimized for good performance. This is accomplished by adapting the antecedent parameters (membership function parameters) and consequent parameters (the polynomial coefficients of the consequent part) so that the root mean square error (RMSE) is minimized as follows [11]:

$$RMSE = \sqrt{\frac{1}{N} \sum_{K=1}^{N} (O_{actual} - O_{predicted})^2} \quad ....(12)$$

Where

O_{actual} and $O_{predicted}$ are the actual and predicted outputs respectively, N is the number of training data.

First and fourth layers are adaptive layers in ANFIS architecture. The premise parameters are in the first layer and consequent parameters in the fourth layer. The task of the learning is to tune these modifiable parameters to make ANFIS output match the training data. To improve the rate of error convergence, a hybrid learning algorithm that combines the least square and gradient descent method is adopted [12]. The fuzzy system parameters are tuned by two steps to minimize the RMSE between the target values and the trained ones. The first and second steps are called forward and backward pass respectively.In the forward pass of hybrid learning algorithm, functional signals go forward till layer 4 and the consequent parameters are identified and optimized by the least squares estimate with the premise parameters fixed [13]. In the backward pass, the error rates propagate backward and the premise parameters are updated by the gradient descent. Once the optimal consequent parameters are found, the gradient descent method is used to adjust optimally the premise parameters corresponding to the fuzzy sets in input domain [12]. The back-propagation algorithm with a gradient descent is a general method for recursively solving parameter optimization. This algorithm can tune the antecedent parameters so that the predefined objective function (RMSE) is minimized [11].

Results and Discussion

In this type of ANFIS prediction, the control factors are the inputs and the roughness values are the output of this system that is based on grid partition for data spacing as shown in Figure (13).

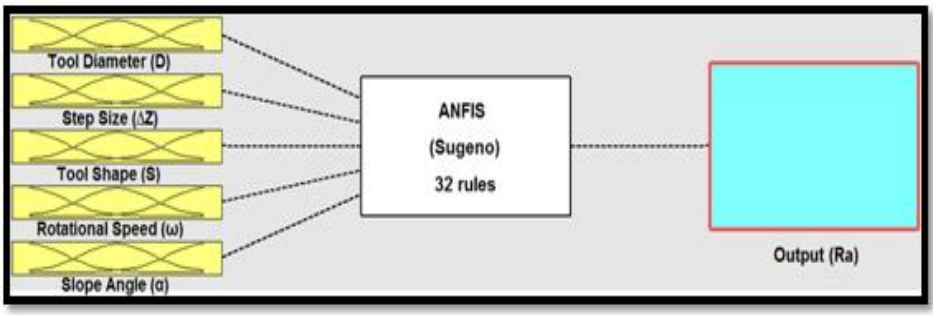

Figure (13): ANFIS input-output mapping.

In order to start modeling ANFIS, a total of 18 experimental data sets shown in Table (3) are randomly selected from the total of 24 experimental sets for the purpose of training the model and the remaining-unseen 6 sets (expt. 4, 6, 11, 13, 19 & 20) are then used for testing after training is completed to verify the accuracy of the predicted values of surface roughness.

By trial and error , the total iterations to select ANFIS parameters are listed in Table (4).

Table (4):Different ANFIS parameters

Input MF	No. of input MFs	Consequent	Training RMSE	Testing RMSE
Gaussian	2	constant	0.034291	0.17182
		linear	0.006338	0.29965
	3	constant	0.022323	0.64722
		linear	0.00026198	0.61397
Two-sided Gaussian	2	constant	0.037792	0.17858
		linear	0.0080046	0.29049
	3	constant	0.022346	0.68858
		linear	0.00015659	0.67624
Triangular	2	constant	0.034512	0.16734
		linear	0.0060195	0.34483
	3	constant	0.022317	0.64932
		linear	$4.5641*10^{-5}$	0.64871
Trapezoidal	2	constant	0.045744	0.61012
		linear	0.010128	0.61108
	3	constant	0.022317	0.67138
		linear	0.00010883	0.6681
Bell-shaped	2	constant	0.034067	0.16921
		linear	0.0067082	0.42079
	3	constant	0.02235	0.62804
		linear	0.00058162	0.58429
Difference sigmoidal	2	constant	0.034005	0.16384
		linear	0.0082619	0.23592
	3	constant	0.022347	0.69374
		linear	0.0001928	0.68033
Product sigmoidal	2	constant	0.03401	0.164
		linear	0.0082594	0.24372
	3	constant	0.022363	0.69099
		linear	0.00013677	0.68033

According to Table (4), the best ANFIS setting that gives the optimal-minimum error is listed in Table (5).

Table (5): ANFIS parameters for roughness prediction model.

ANFIS Parameter	Details
Data Spacing	Grid partition
MF type	Difference sigmoidal
No. of input MFs	2
Consequent part	Constant (zero order system)
Error optimization	Hybrid learning algorithm

As the number of inputs and MFs for each input are 5 and 2 respectively; then the number of fuzzy rules for this system using grid partitioning method is (2^5 = 32 rules). Since each input is fuzzified into two fuzzy sets or membership grades (μ): high and low; then thefuzzy rules of ANFIS can be written in terms of these grades as shown in Table (6). The corresponding ANFIS structure can be found in appendix 1.

Table (6): Fuzzy rules of ANFIS

Rule No.	If					Then
	μ (D)	μ (ΔZ)	μ (S)	μ (ω)	μ (α)	Ra
1	Low	Low	Low	Low	Low	Level 1
2	Low	Low	Low	Low	High	Level 2
3	Low	Low	Low	High	Low	Level 3
4	Low	Low	Low	High	High	Level 4
5	Low	Low	High	Low	Low	Level 5
6	Low	Low	High	Low	High	Level 6
7	Low	Low	High	High	Low	Level 7
8	Low	Low	High	High	High	Level 8
9	Low	High	Low	Low	Low	Level 9
10	Low	High	Low	Low	High	Level 10
11	Low	High	Low	High	Low	Level 11
12	Low	High	Low	High	Low	Level 12
13	Low	High	High	Low	High	Level 13
14	Low	High	High	Low	Low	Level 14
15	Low	High	High	High	High	Level 15
16	Low	High	High	High	Low	Level 16
17	High	Low	Low	Low	High	Level 17
18	High	Low	Low	Low	Low	Level 18
19	High	Low	Low	High	High	Level 19
20	High	Low	Low	High	Low	Level 20
21	High	Low	High	Low	High	Level 21
22	High	Low	High	Low	Low	Level 22
23	High	Low	High	High	Low	Level 23
24	High	Low	High	High	High	Level 24
25	High	High	Low	Low	Low	Level 25
26	High	High	Low	Low	High	Level 26
27	High	High	Low	High	Low	Level 27
28	High	High	Low	High	High	Level 28
29	High	High	High	Low	Low	Level 29
30	High	High	High	Low	High	Level 30
31	High	High	High	High	Low	Level 31
32	High	High	High	High	High	Level 32

By utilizing the training data with hybrid optimization algorithm through the setting shown in Table (5), ANFIS training process starts minimizing the error gradually until reaching the situation of error constancy which represents the smallest obtainable error as shown in Figure (14). The minimal root mean square error (RMSE) reached by using difference sigmoidal MF within 300 epochs is 0.034005. Consequently, the testing RMSE using testing data is 0.16384.

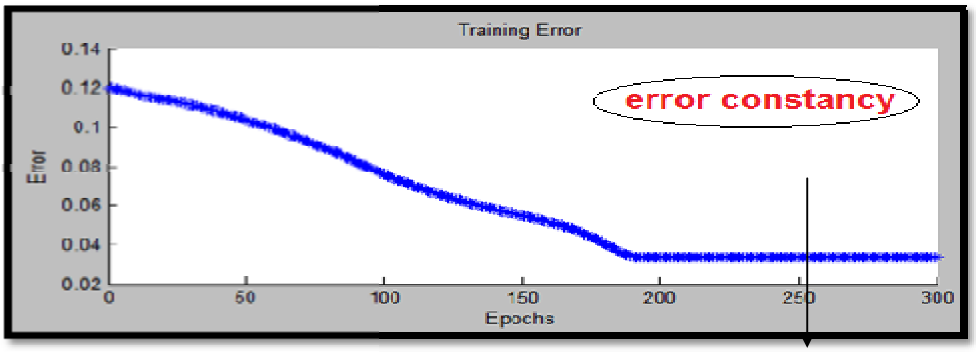

Figure (14): ANFIS training process.

After the construction of ANFIS model is completed, a plot of the difference sigmoidal membership functions for each input variable can be shown in figure (15).

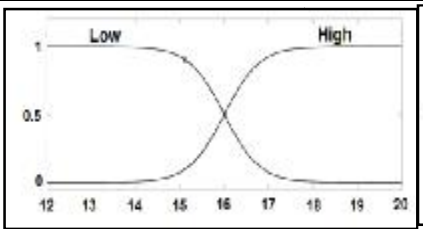

(a) Input variable "Diameter"

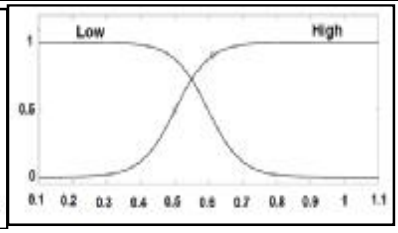

(b) Input variable "Step size"

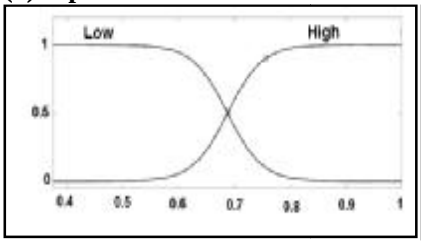

(c) Input variable "Tool shape"

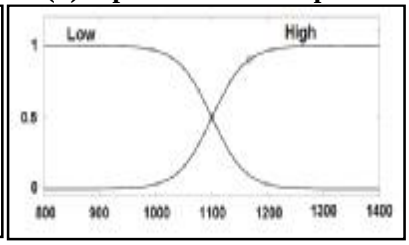

(d) Input variable "Rotational speed"

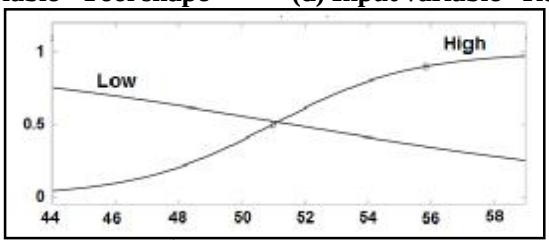

(e) Input variable "Slope angle"

Figure (15): ANFIS membership functions for inputs.

The optimal premise and consequent parameters of ANFIS rules that correspond to the previous membership functions (Figure (15)) can be obtained. These parameters are listed in Table (7) & (8) respectively.

Table (7): Optimal premise parameters for difference sigmoidal MF.

Input variable	Grade	Premise parameters			
		a_1	c_1	a_2	c_2
D	Low	2.5	8	2.5	16
	High	2.5	16	2.5	24
ΔZ	Low	20	-0.4	20	0.5981
	High	20	0.5014	20	1.6
S	Low	32	0.0625	32	0.6875
	High	32	0.6875	32	1.312
ω	Low	0.03333	500	0.03333	1100
	High	0.03333	1100	0.03333	1700
α	Low	1.333	36.5	0.1483	51.59
	High	0.4537	50.98	1.333	66.5

Table (8): Optimal consequent parameters for difference sigmoidal MF.

Rule No.	Consequent Parameters	Rule No.	Consequent Parameters	Rule No.	Consequent Parameters
1	1.081	**12**	0.837	**23**	0.2566
2	0.4832	**13**	1.296	**24**	0.1708
3	0.5543	**14**	0.764	**25**	1.391
4	0.2214	**15**	2.263	**26**	0.8606
5	0.7545	**16**	1.046	**27**	1.436
6	0.3189	**17**	0.4989	**28**	0.9005
7	0.4836	**18**	0.2075	**29**	0.8768
8	0.202	**19**	0.4351	**30**	0.4965
9	3.207	**20**	0.1958	**31**	1.231
10	0.8988	**21**	0.3087	**32**	0.4053
11	4.494	**22**	0.1967		

According to the previous structure and optimal parameters of ANFIS, the predicted results using both training and testing data are shown in Tables (9) and (10) respectively.

Table (9): Experimental prediction results using training data.

Expt. No.	α	Actual R_a	Predicted R_a	Absolute error %	Expt. No.	α	Actual R_a	Predicted R_a	Absolute error %
1	59	0.6	0.605	0.833	14	59	0.24	0.242	0.833
	54	0.74	0.687	7.162		54	0.27	0.273	1.111
	49	0.84	0.886	5.476		49	0.36	0.35	2.777
	44	1.08	1.05	2.777		44	0.37	0.413	11.621
2	59	0.24	0.29	20.833	15	59	0.2	0.22	10
	54	0.39	0.335	14.102		54	0.26	0.235	9.615
	49	0.46	0.446	3.043		49	0.27	0.272	0.74
	44	0.52	0.539	3.653		44	0.3	0.303	1
3	59	0.44	0.467	6.136	16	59	0.18	0.188	4.444
	54	0.42	0.408	2.857		54	0.21	0.2	4.761
	49	0.64	0.612	4.375		49	0.23	0.229	0.434
	44	0.72	0.733	1.805		44	0.25	0.253	1.2
5	59	0.68	0.686	0.882	17	59	0.33	0.337	2.121
	54	0.78	0.792	1.538		54	0.4	0.378	5.5
	49	1.03	1.05	1.941		49	0.45	0.48	6.666
	44	1.27	1.27	0		44	0.58	0.565	2.586
7	59	0.43	0.457	6.279	18	59	0.31	0.32	3.225
	54	0.54	0.518	4.074		54	0.38	0.356	6.315
	49	0.69	0.666	3.478		49	0.42	0.444	5.714
	44	0.77	0.789	2.467		44	0.57	0.517	9.298
8	59	0.38	0.369	2.894	21	59	0.94	0.985	4.787
	54	0.42	0.421	0.238		54	1.07	1.02	4.672
	49	0.52	0.547	5.192		49	1.2	1.19	0.833
	44	0.67	0.653	2.537		44	1.32	1.34	1.515
9	59	1.42	1.37	3.521	22	59	0.9	0.946	5.111
	54	2.08	2.08	0		54	1.13	1.06	6.194
	49	2.51	2.45	2.39		49	1.21	1.24	2.479
	44	3.07	3.09	0.651		44	1.4	1.4	0
10	59	1.58	1.58	0	23	59	0.49	0.574	17.142
	54	1.6	1.68	5		54	0.75	0.752	0.266
	49	3.31	3.3	0.302		49	0.73	0.626	14.246
	44	4.3	4.31	0.232		44	0.84	0.858	2.142
12	59	1.3	1.29	0.769	24	59	0.56	0.574	2.5
	54	1.46	1.46	0		54	0.74	0.686	7.297
	49	1.85	1.86	0.54		49	0.88	0.961	9.204
	44	2.21	2.2	0.452		44	1.23	1.19	3.252
Average error %									**4.028**

Table (10): Experimental prediction results using testing data.

Expt. No.	α	Actual R_a	Predicted R_a	Absolute error %
4	**59**	0.21	0.26	23.809
	54	0.24	0.298	24.166
	49	0.31	0.392	26.451
	44	0.4	0.47	17.5
6	**59**	0.6	0.52	13.333
	54	0.59	0.426	27.796
	49	0.68	0.747	9.852
	44	1.17	0.937	19.914
11	**59**	1.3	0.945	27.307
	54	1.27	0.873	31.259
	49	1.41	1.12	20.567
	44	1.67	1.27	23.952
13	**59**	0.31	0.265	14.516
	54	0.31	0.303	2.258
	49	0.43	0.396	7.906
	44	0.45	0.474	5.333
19	**59**	0.25	0.257	2.8
	54	0.3	0.276	8
	49	0.32	0.323	0.937
	44	0.39	0.362	7.179
20	**59**	0.25	0.229	8.4
	54	0.28	0.252	10
	49	0.32	0.306	4.375
	44	0.34	0.351	3.235
Average error %				**14.201**

As mentioned previously, the training and testing RMSE within 300 epochs are 0.034005 & 0.16384 respectively by using both the training and testing data when difference sigmoidal membership function with two MFs for each input parameter and a zero order output are adopted. As a result, the average-absolute training and testing error are 4.028% (95.972% prediction accuracy) and 14.201% (85.799% prediction accuracy) respectively. The predicted roughness values versus the actual ones using both the training and testing data through the proposed ANFIS model are shown in Figure (16).

Figure (16-b) shows that the predicted roughness generally diverges from the actual one as the magnitude of roughness increases. The maximum absolute error obtained by testing data is 31.259%. The problem of this deviation is because of the high dependency of roughness on the forming parameters which have a small number of levels for each parameter.

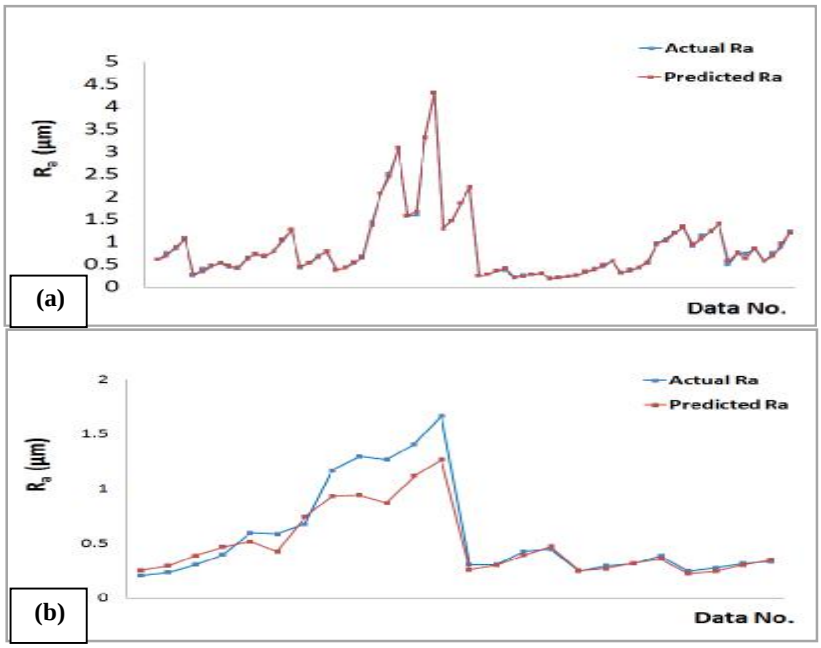

Figure (16): Deviation between actual and predicted R_a byANFIS using: (a) training data, (b) testing data.

Conclusions

The proposed ANFIS model is a successful approach to establish the relationship between the actual surface roughness as the output and the forming parameters (tool diameter, step size, tool shape, rotational speed and slope angle) as the inputs of this estimation method of roughness in SPIF process. Once these forming parameters are given, then the estimated surface roughness (R_a) can be easily obtained. Experimental results show that the difference sigmoidal MF with constant output gives the minimum RMSE. The predicted surface roughness values using ANFIS are compared with actual data. The comparison indicates that the utilization of difference sigmoidal MF in ANFIS could achieve a satisfactory prediction accuracy using both training and testing data when this MF is adopted. The training and testing prediction accuracy are 95.972% and 85.799% respectively.

Appendix -1-

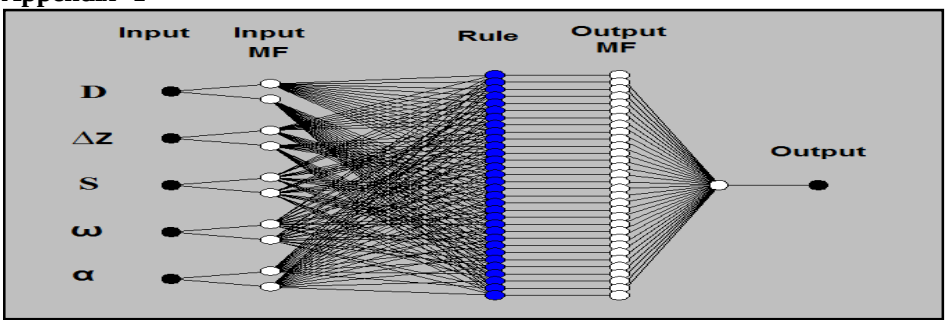

- ANFIS Structure -

REFERENCES

[1].N. Satheesh Kumar, Ajay Shetty, Ashay Shetty, Ananth K & Harsha Shettyba "Effect of spindle speed and feed rate on surface roughness of Carbon Steels in CNC turning" Procedia Engineering. Vol. 38 pp. 691 – 697, 2012.

[2].V. Oleksik, A. Pascu, C. Deac, R. Fleacă, O. Bologa & G. Racz "Experimental Study on the Surface Quality of the Medical Implants Obtained By Single Point Incremental Forming" Int J Mater Form. Vol. 3, pp. 935-938, 2010.

[3].Alexandru C. Filip & Ion Neagoe1 "An Overview on Incremental Sheet Forming, A Method for Rapid Manufacturing of Hollow Metal Parts" Academic Journal of Manufacturing Engineering. Vol. 8, pp. 24-29, 2010.

[4].Salah B. M. Echrif & Meftah Hrairi "Process Simulation and Quality Evaluation of Incremental Sheet Forming" IIUM Engineering Journal, Special Issue, Mechanical Engineering. pp. 185-196, 2011.

[5].A. Attanasio, E. Ceretti, C. Giardini & L. Mazzoni "Asymmetric two points incremental forming: Improving surface quality and geometric accuracy by tool path optimization" Journal of Materials Processing Technology. Vol. 197, pp. 59–67, 2008.

[6].Zemin Fu, Jianhua Mo, Fei Han & Pan Gong " Tool path correction algorithm for single-point incremental forming of sheet metal" Int J Adv Manuf Technol. Vol. 64, pp. 1239–1248, 2013.

[7].S.H.Wu1, Ana Reis, F.M. Andrade Pires, Abel D. Santos & A. Barata da Rocha " Study of tool trajectory in incremental forming" Advanced Materials Research. Vols. 472-475, pp. 1586-1591, 2012.

[8].Radu Crina & Vasile Alecsandri "New Configurations of the SPIF Process - A Review" Journal of Engineering Studies and Research. Vol. 16, pp. 33-39, 2010.

[9].Ulas Caydas, Ahmet Hascalik & Sami Ekici "An adaptive neuro-fuzzy inference system (ANFIS) model for wire-EDM" Expert Systems with Applications. Vol. 36, pp. 6135-6139, 2009.

[10].B. Sidda Reddy, J. Suresh Kumar & K. Vijaya Kumar Reddy "Prediction of Surface Roughness in Turning Using Adaptive Neuro-Fuzzy Inference System" Jordan Journal of Mechanical and Industrial Engineering. Vol. 3, pp. 252-259, 2009.

[11].M. G. Na "DNB Limit Estimation Using an Adaptive Fuzzy Inference System" IEEE Transactions on Nucleax Science. Vol. 47, pp. 1948-1953, 2000.

[12]./Shibendu Shekhar Roy "Design of adaptive neuro-fuzzy inference system for predicting surface roughness in turning operation" Journal of Scientific & Industrial Research. Vol. 64, pp. 653-659, 2005.

[13].S.R. Nikam, P.J.Nikumbh & S.P.Kulkarni "Fuzzy Logic and Neuro Fuzzy Modeling" International Journal of Computer Applications. Vol. NCRTC, pp. 22-31, 2012.